Supporting Information

for

High Affinity Crown Ether Complexes in Water: Thermodynamic Analysis, Evidence of Crystallography and Binding of NAD^+

Ling Chen, Heng-Yi Zhang, and Yu Liu*

Department of Chemistry, State Key Laboratory of Elemento-Organic Chemistry, Nankai University, Tianjin 300071, People's Republic of China

yuliu@nankai.edu.cn

Table of Contents

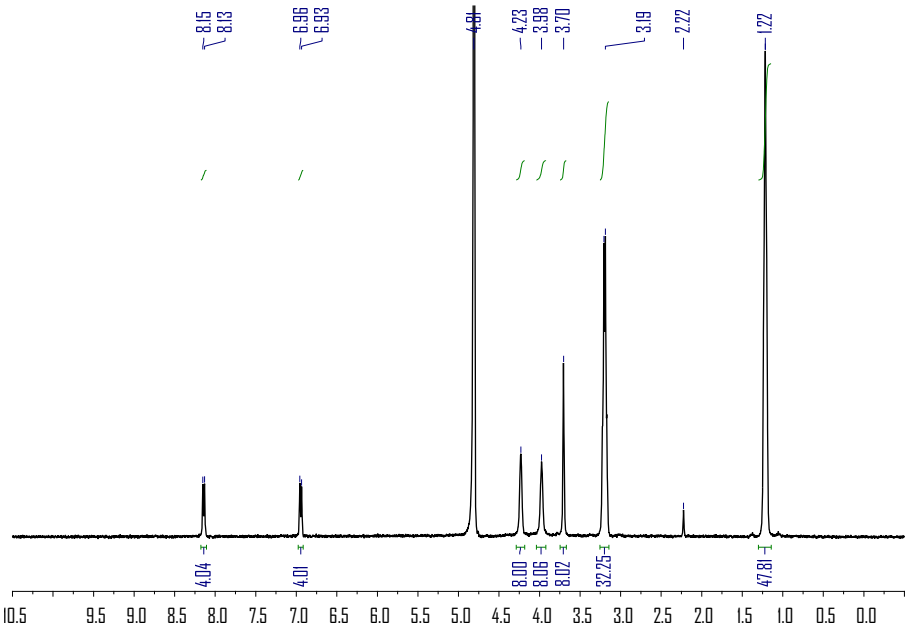

Figure S1. ^{1}H NMR spectrum of $(NEt_4)_4$·**1** (D_2O, 400 MHz, 25 °C).

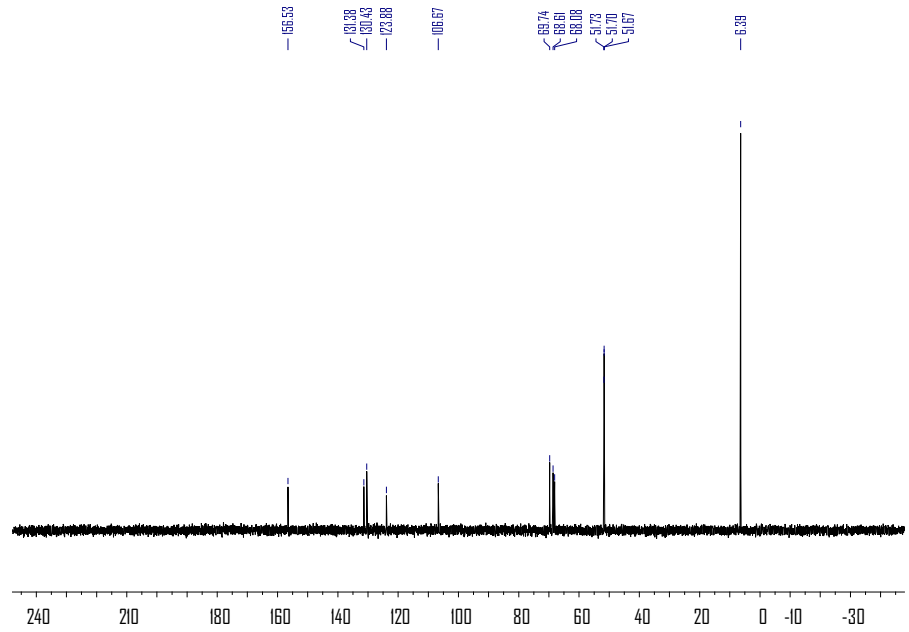

Figure S2. ^{13}C NMR spectrum of $(NEt_4)_4$·**1** (D_2O, 100 MHz, 25 °C).

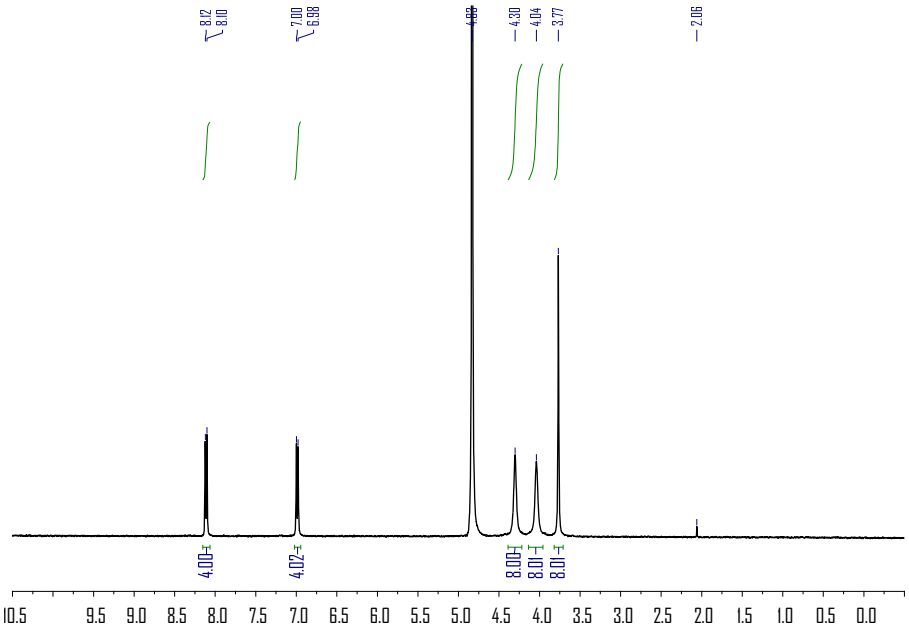

Figure S3. ^{1}H NMR spectrum of Na_4·**1** (D_2O, 400 MHz, 25 °C).

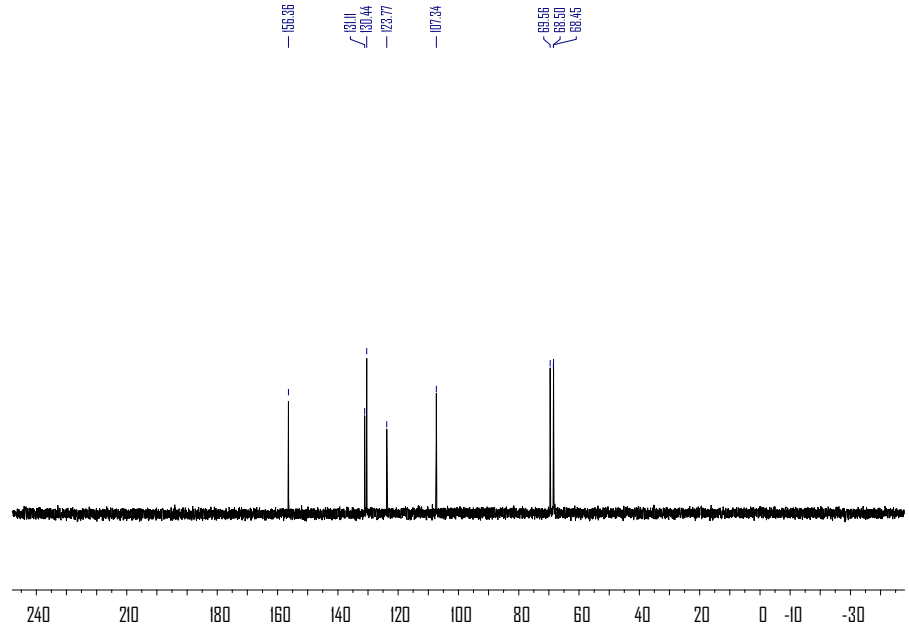

Figure S4. ^{13}C NMR spectrum of Na_4·**1** (D_2O, 100 MHz, 25 °C).

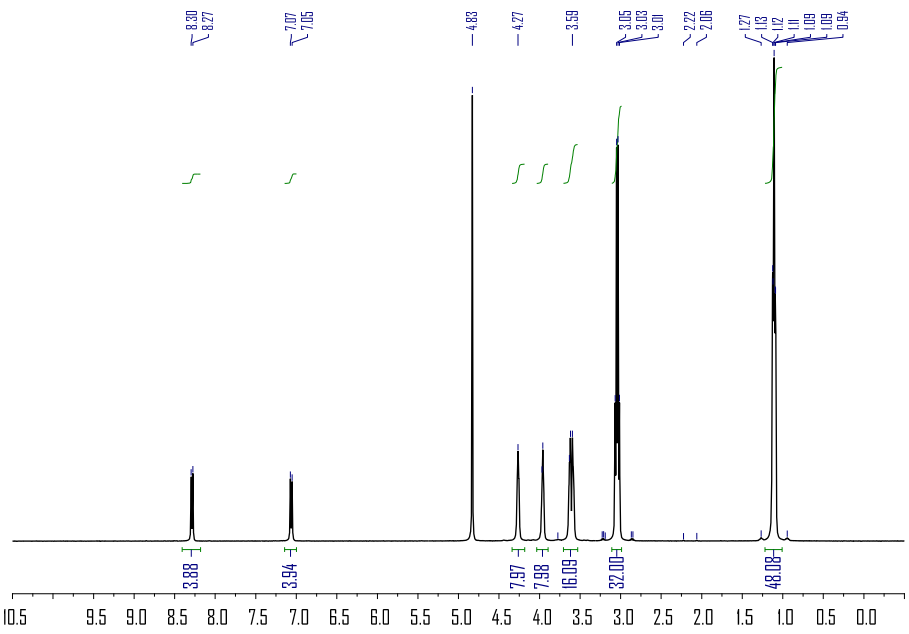

Figure S5. ^{1}H NMR spectrum of $(NEt_4)_4$·**2** (D_2O, 400 MHz, 25 °C).

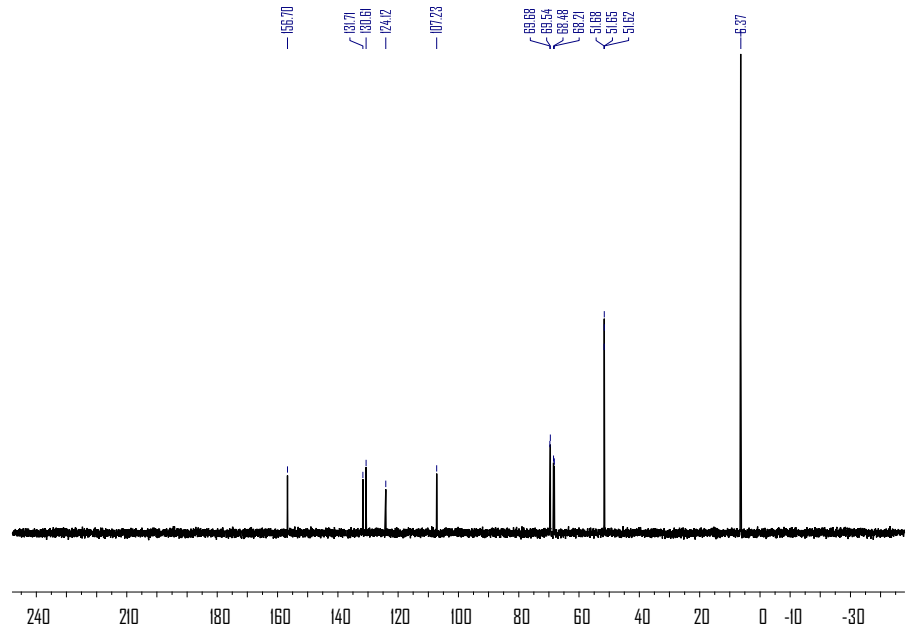

Figure S6. ^{13}C NMR spectrum of $(NEt_4)_4$·**2** (D_2O, 100 MHz, 25 °C).

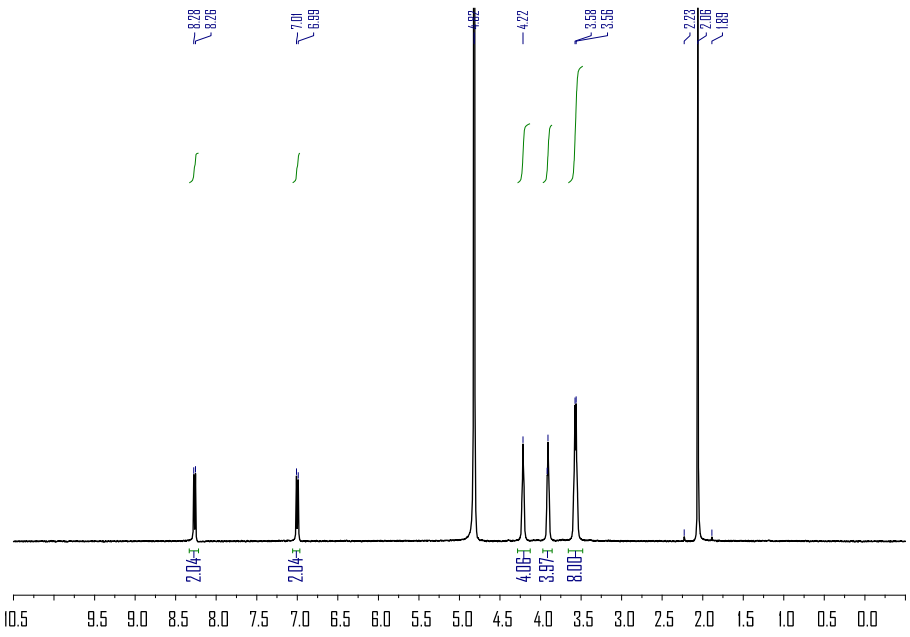

Figure S7. ^{1}H NMR spectrum of Na_4·**2** (D_2O, 400 MHz, 25 °C).

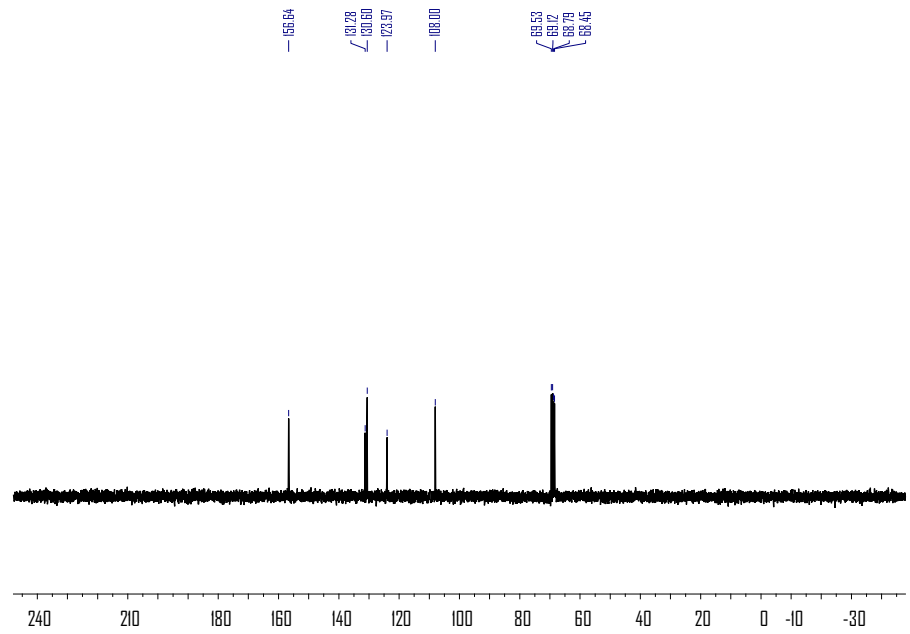

Figure S8. ^{13}C NMR spectrum of Na_4·**2** (D_2O, 100 MHz, 25 °C).

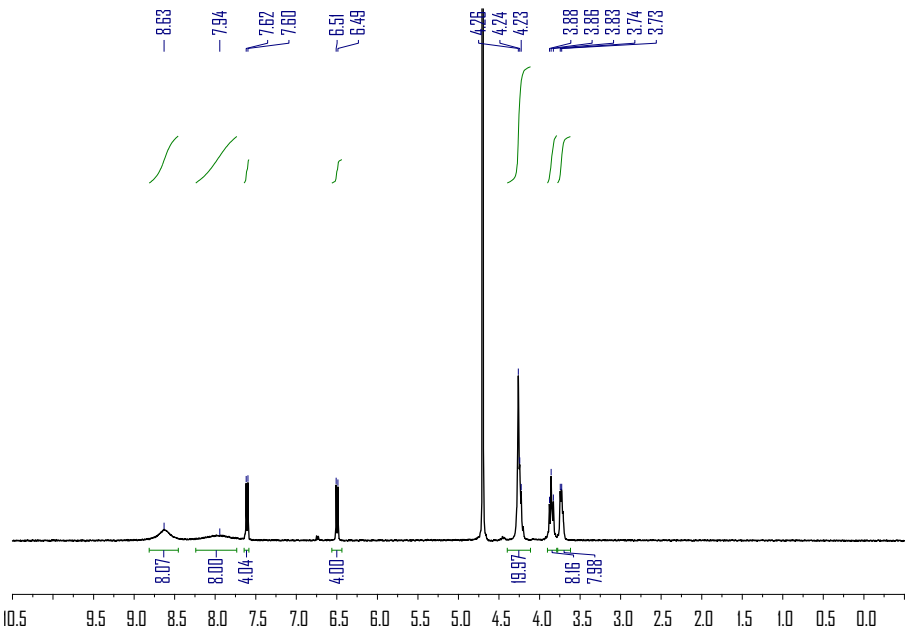

Figure S9. ^{1}H NMR spectrum of $\mathbf{3}_2\cdot\mathbf{1}$ (D_2O, 400 MHz, 25 °C).

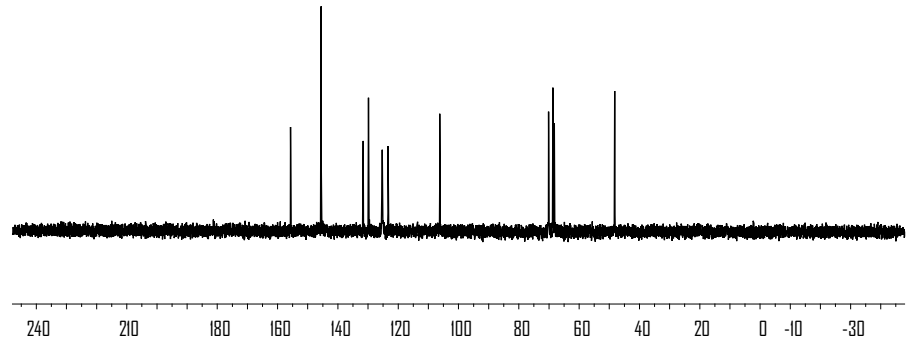

Figure S10. ^{1}H NMR spectrum of $\mathbf{3}_2\cdot\mathbf{1}$ (D_2O, 100 MHz, 25 °C).

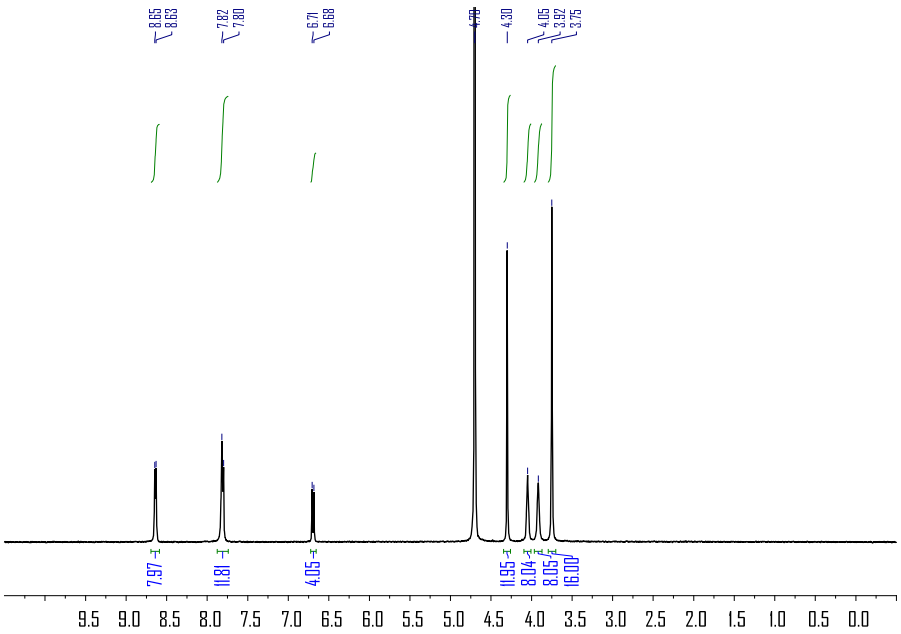

Figure S11. ^{1}H NMR spectrum of $\mathbf{3}_2\cdot\mathbf{2}$ (D_2O, 400 MHz, 25 °C).

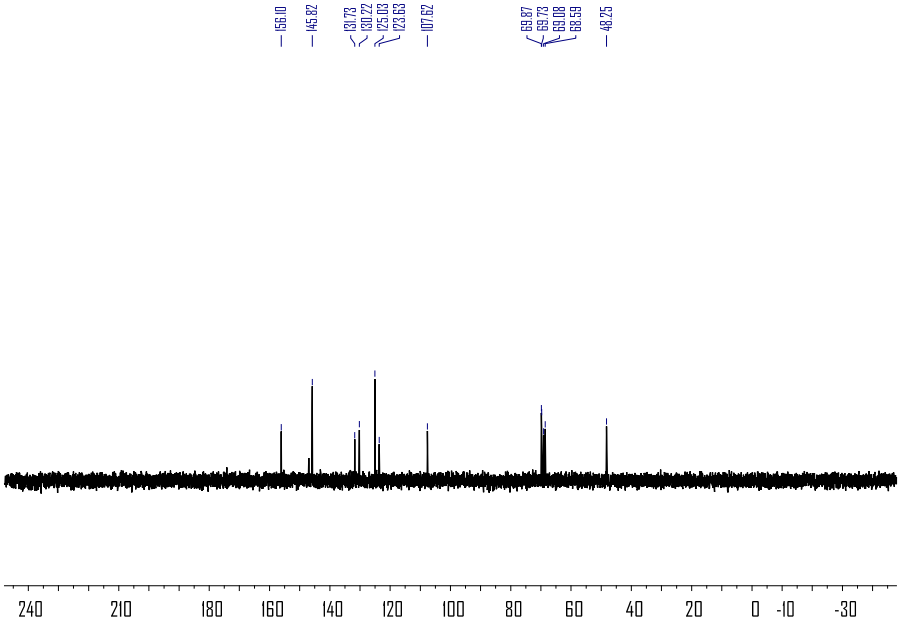

Figure S12. ^{13}C NMR spectrum of $\mathbf{3}_2\cdot\mathbf{2}$ (D_2O, 100 MHz, 25 °C).

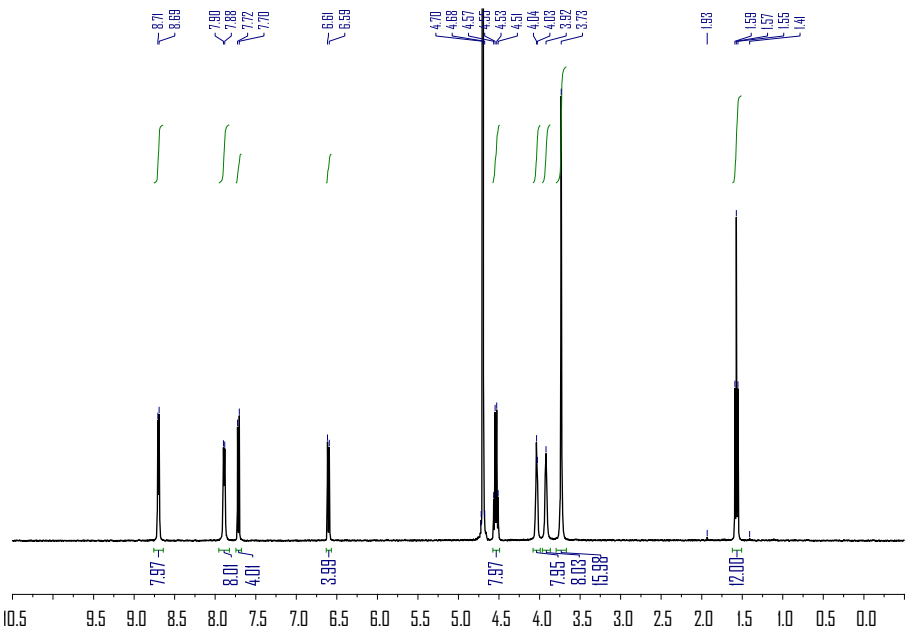

Figure S13. ^{1}H NMR spectrum of $\mathbf{4}_2\cdot\mathbf{2}$ (D_2O, 400 MHz, 25 °C).

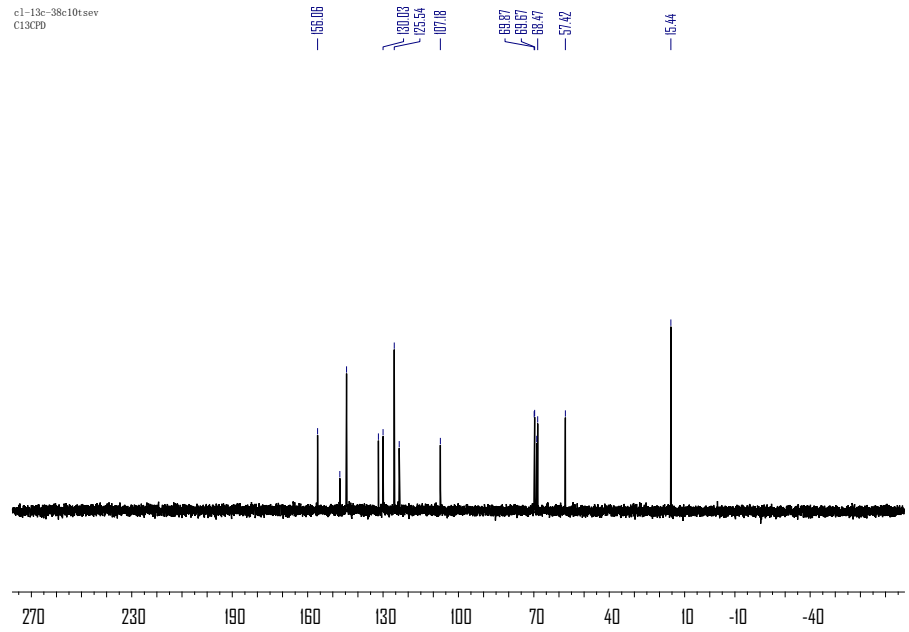

Figure S14. ^{1}H NMR spectrum of $\mathbf{4}_2\cdot\mathbf{2}$ (D_2O, 100 MHz, 25 °C).

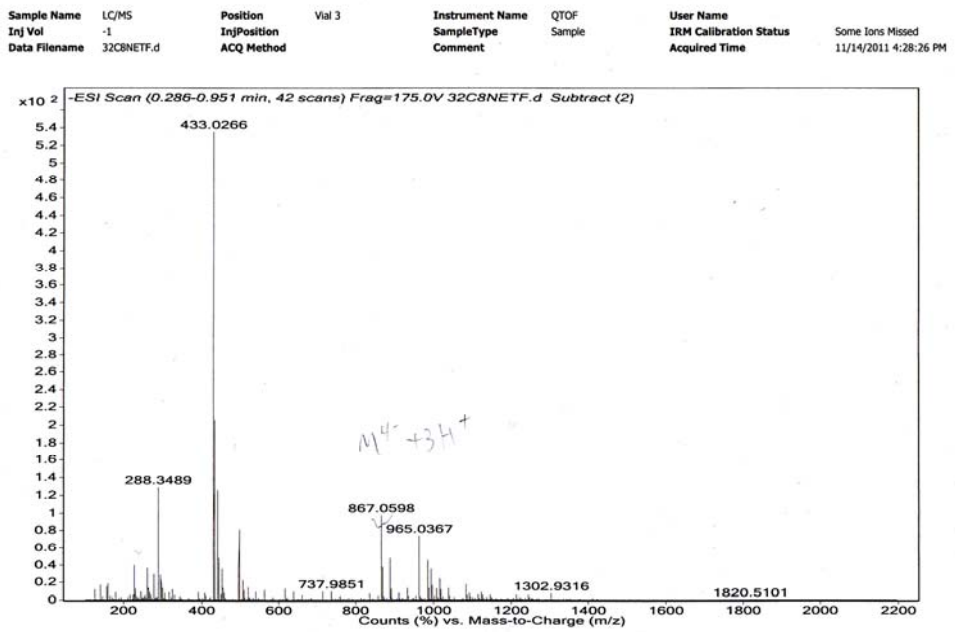

Figure S15. ESI-MS spectrum of $(NEt_4)_4$·**1**.

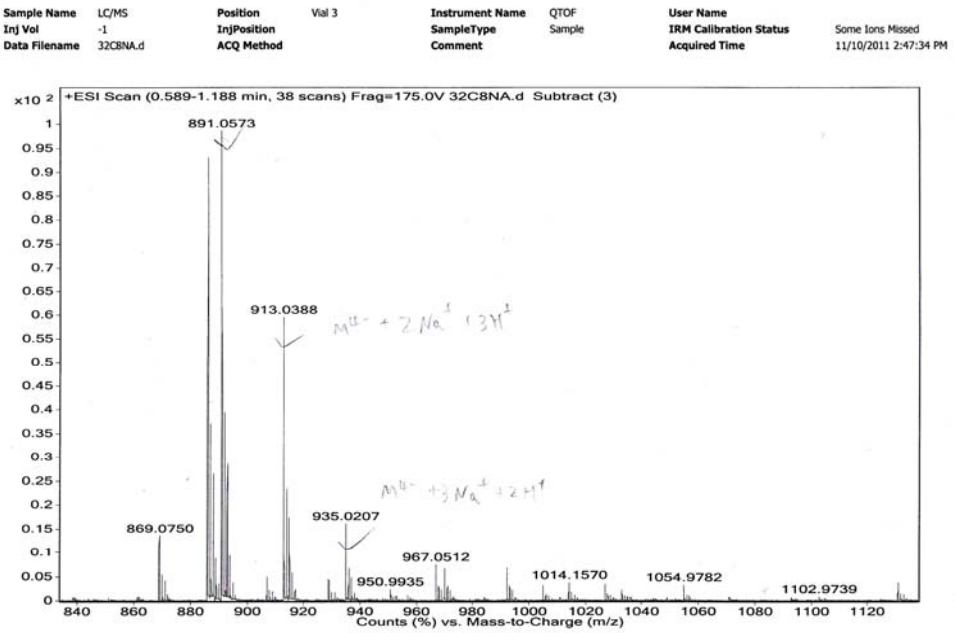

Figure S16. ESI-MS spectrum of Na_4·**1**.

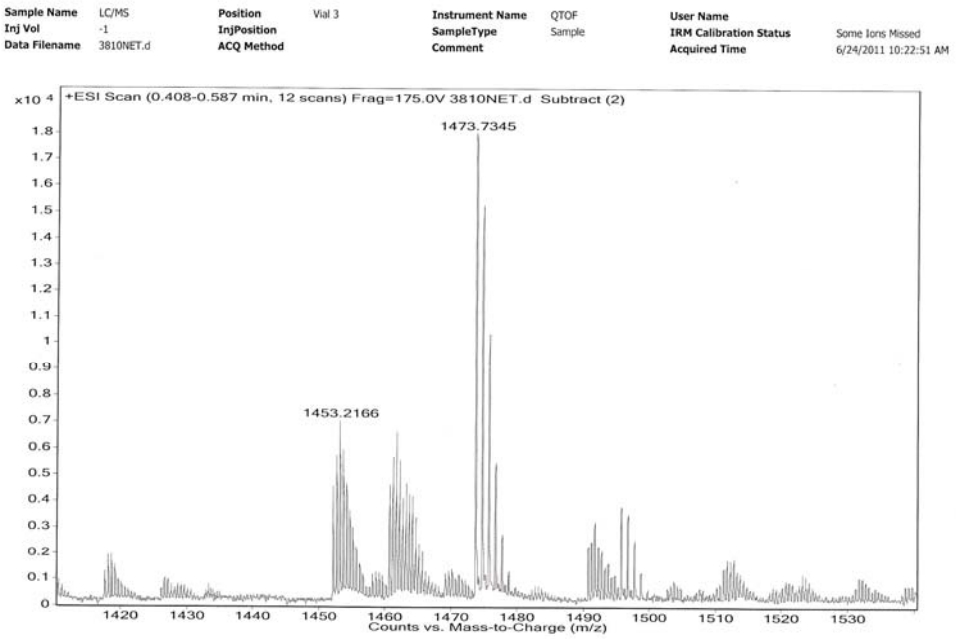

Figure S17. ESI-MS spectrum of $(NEt_4)_4$·**2**.

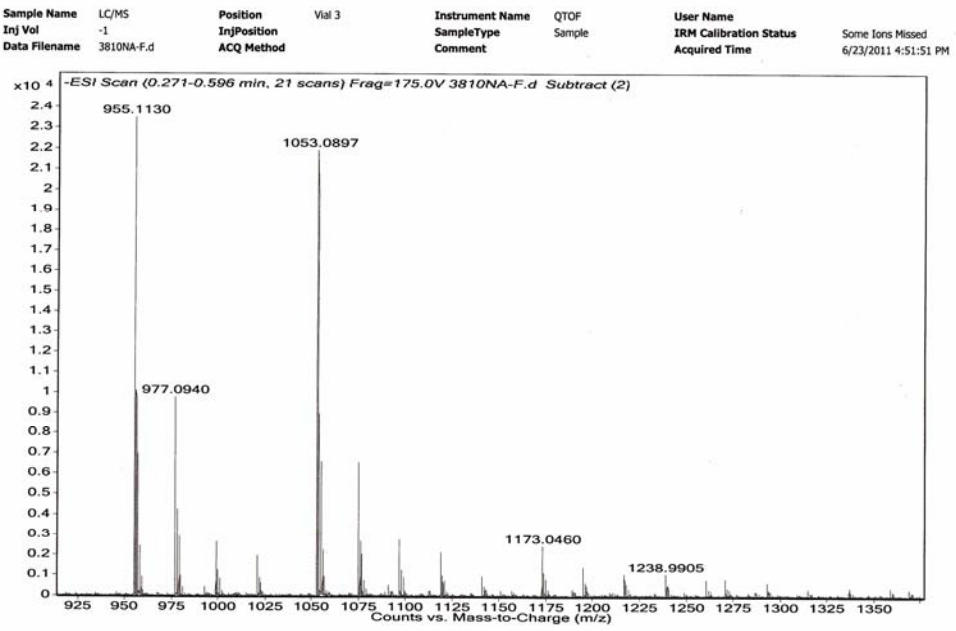

Figure S18. ESI-MS spectrum of Na_4·**2**.

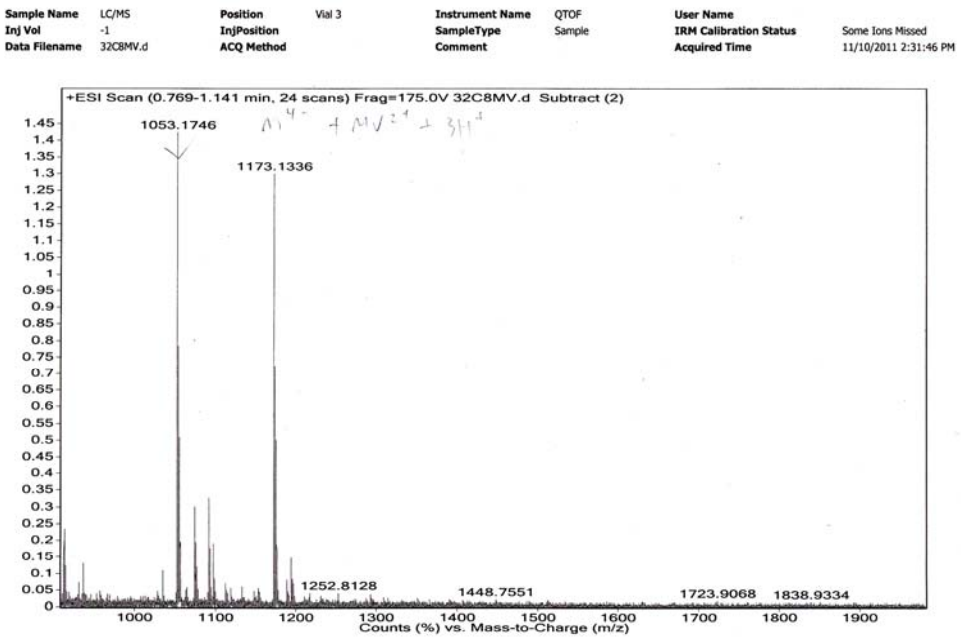

Figure S19. ESI-HRMS spectrum of $\mathbf{3}_2\cdot\mathbf{1}$.

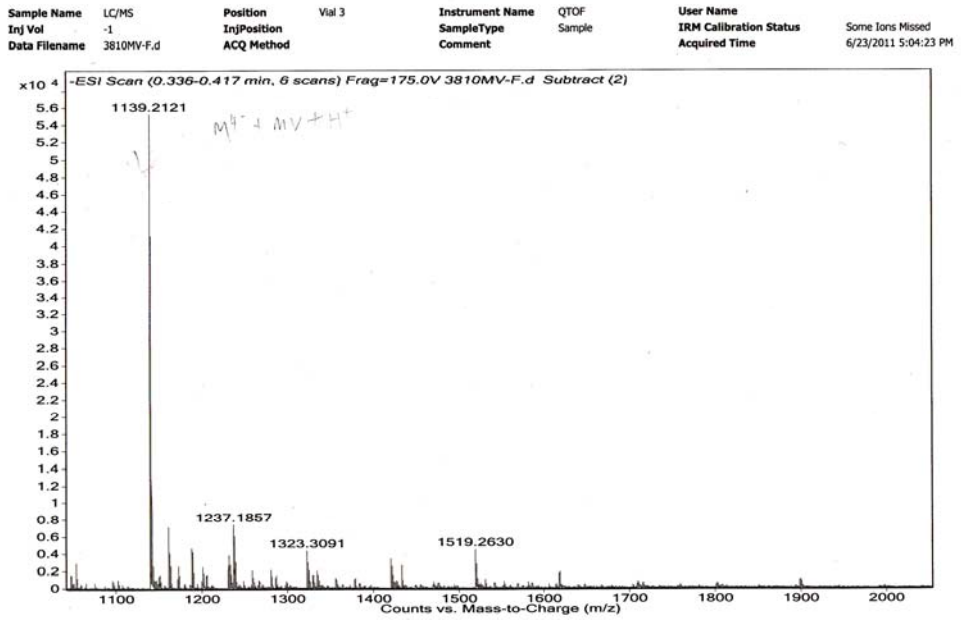

Figure S20. ESI-MS spectrum of $\mathbf{3}_2\cdot\mathbf{2}$.

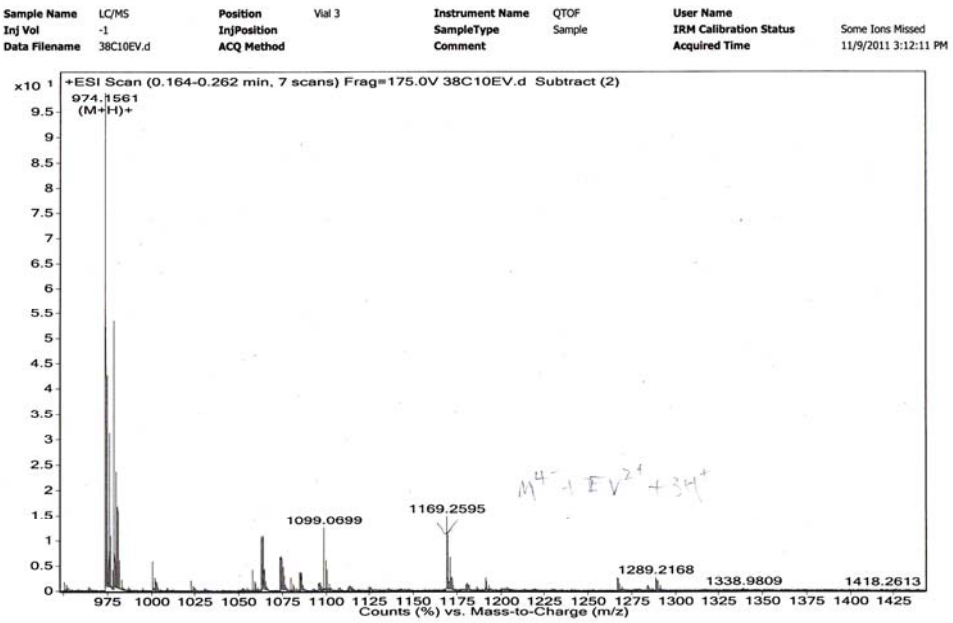

Figure S21. ESI-HRMS spectrum of $\mathbf{4}_2\cdot\mathbf{2}$.

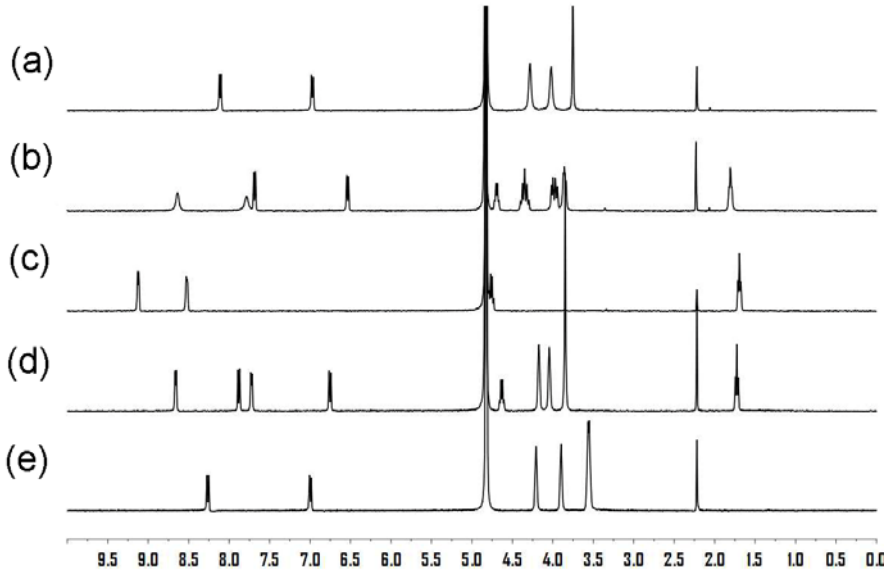

Figure S22. Partial ^{1}H NMR spectrum (400 MHz, D_2O, 25 °C) of (a) free host $Na_4\cdot\mathbf{1}$ ([$Na_4\cdot\mathbf{1}$] = 2 mM); (b) $\mathbf{4}\cdot Br_2$ and equiv $Na_4\cdot\mathbf{1}$ ([$\mathbf{4}\cdot Br_2$] = [$Na_4\cdot\mathbf{1}$] = 2 mM); (c) free guest $\mathbf{4}\cdot Br_2$ ([$\mathbf{4}\cdot Br_2$] = 2 mM); (d) $\mathbf{4}\cdot Br_2$ and equiv $Na_4\cdot\mathbf{2}$ ([$\mathbf{4}\cdot Br_2$] = [$Na_4\cdot\mathbf{2}$] = 2 mM); (c) free host host $Na_4\cdot\mathbf{2}$ ([$Na_4\cdot\mathbf{2}$] = 2 mM).

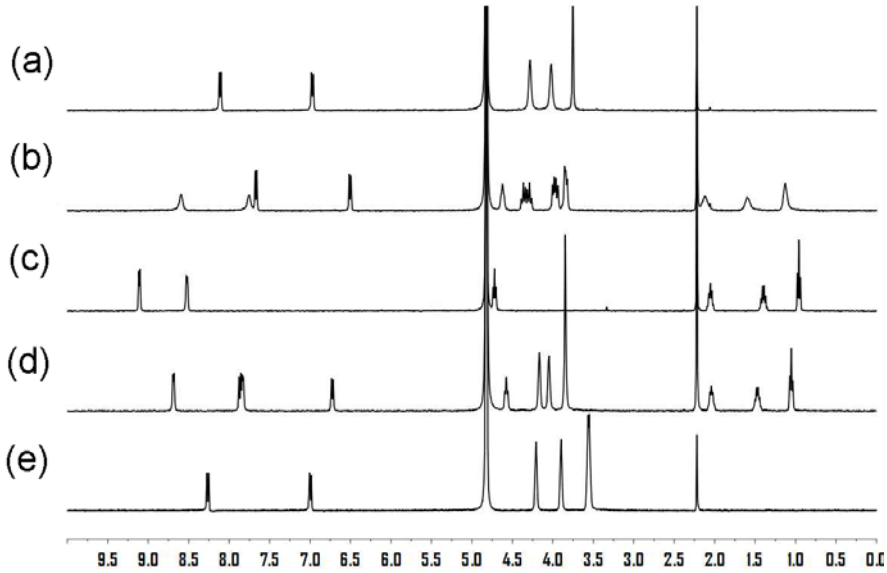

Figure S23. Partial ^{1}H NMR spectrum (400 MHz, D_2O, 25 °C) of (a) free host Na_4·**1** ([Na_4·**1**] = 2 mM); (b) **5**·Br_2 and equiv Na_4·**1** ([**5**·Br_2] = [Na_4·**1**] = 2 mM); (c) free guest **5**·Br_2 ([**5**·Br_2] = 2 mM); (d) **5**·Br_2 and equiv Na_4·**2** ([**5**·Br_2] = [Na_4·**2**] = 2 mM); (c) free host host Na_4·**2** ([Na_4·**2**] = 2 mM).

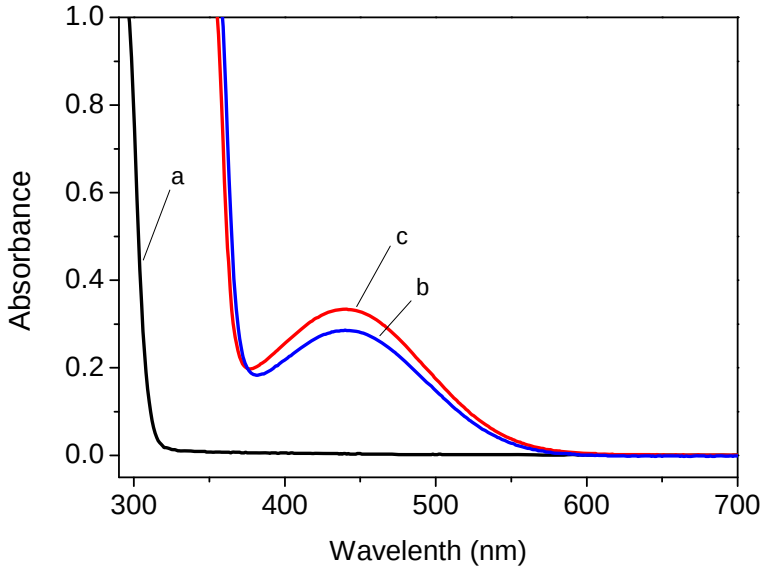

Figure 24. UV-vis absorption spectrum of (a) **4**·Br_2 (1 mM), (b) **4**·Br_2 (1 mM) + Na_4·**1** (1 mM), and (c) **4**·Br_2 (1 mM) + Na_4·**2** (1 mM).

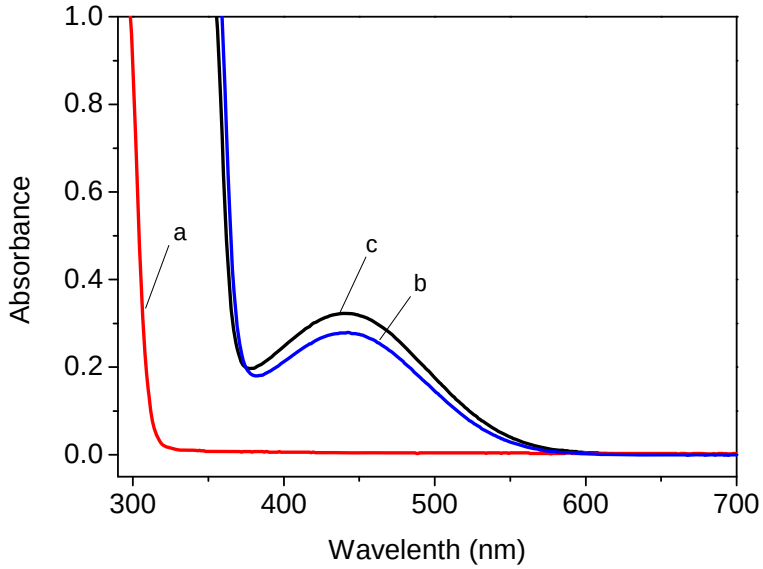

Figure 25. UV-vis absorption spectrum of (a) **5**·Br_2 (1 mM), (b) **5**·Br_2 (1 mM) + Na_4·**1** (1 mM), and (c) **5**·Br_2 (1 mM) + Na_4·**2** (1 mM).

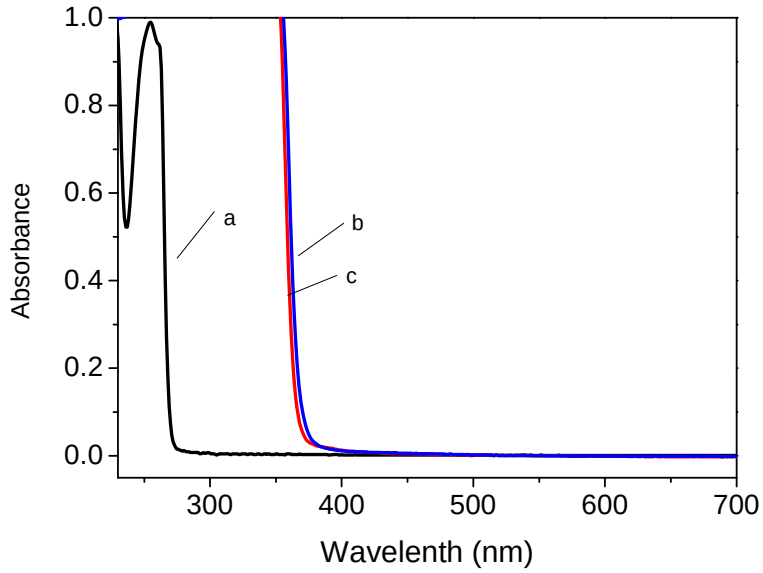

Figure 26. UV-vis absorption spectrum of (a) **6**·Br (1 mM), (b) **6**·Br (1 mM) + Na_4·**1** (1 mM), and (c) **6**·Br (1 mM) + Na_4·**2** (1 mM).

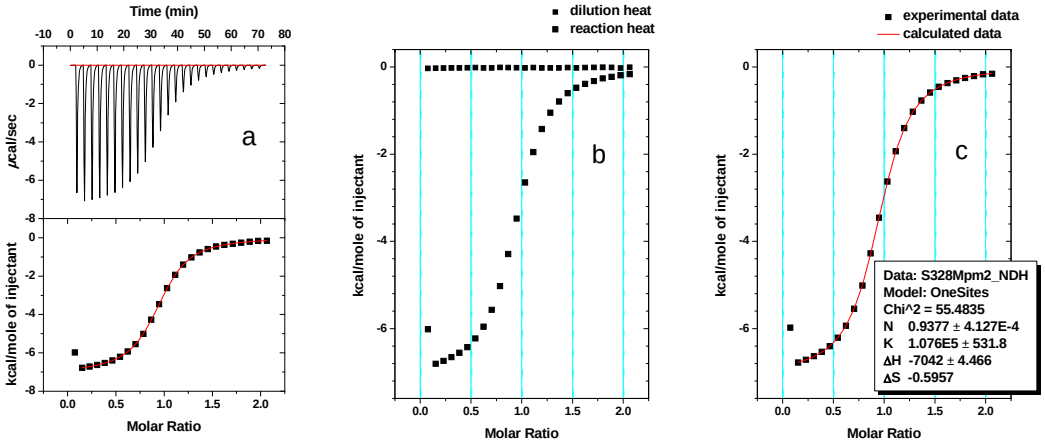

Figure S27. Calorimetric titrations for sequential 25 injections (10 µL per injection) of **6**·Br solution (3.113 mM) injecting into Na_4·**1** solution (0.2630 mM): (a) raw data and apparent reaction heat; (b) heat effects of the dilution and of the complexation reaction; (c) "Net" heat effects fitted using the "one set of binding sites" model.

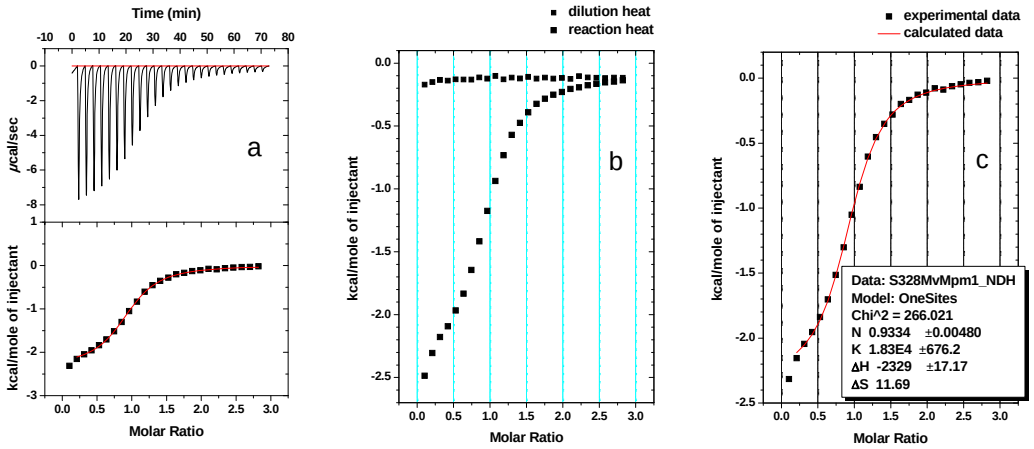

Figure S28. Calorimetric titrations for sequential 25 injections (10 µL per injection) of **3**·Br_2 solution (11.96 mM) injecting into Na_4·**1** solution (0.8098 mM) in the presence of **6**·Br (20.22 mM) as competitor: (a) raw data and apparent reaction heat; (b) heat effects of the dilution and of the complexation reaction; (c) "Net" heat effects fitted using the "one set of binding sites" model.

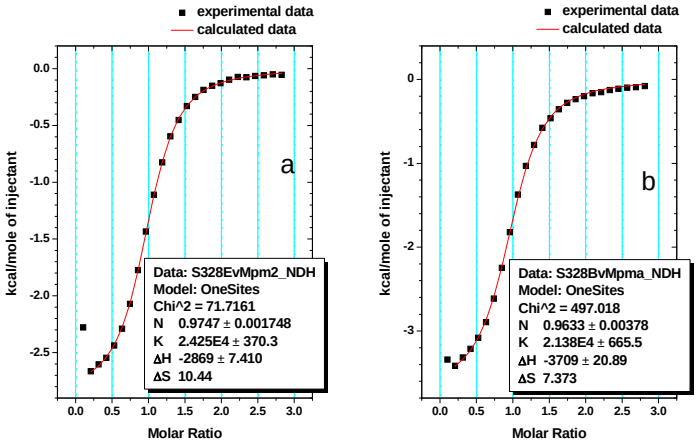

Figure S29. Competition ITC experiment on complexation of **4**·Br_2 (11.98 mM) and **5**·Br_2 (11.91 mM) with Na_4·**1** (0.8098 mM) in the presence of **6**·Br (20.22 mM) as competitor: (a) **4**·Br_2; (b) **5**·Br_2.

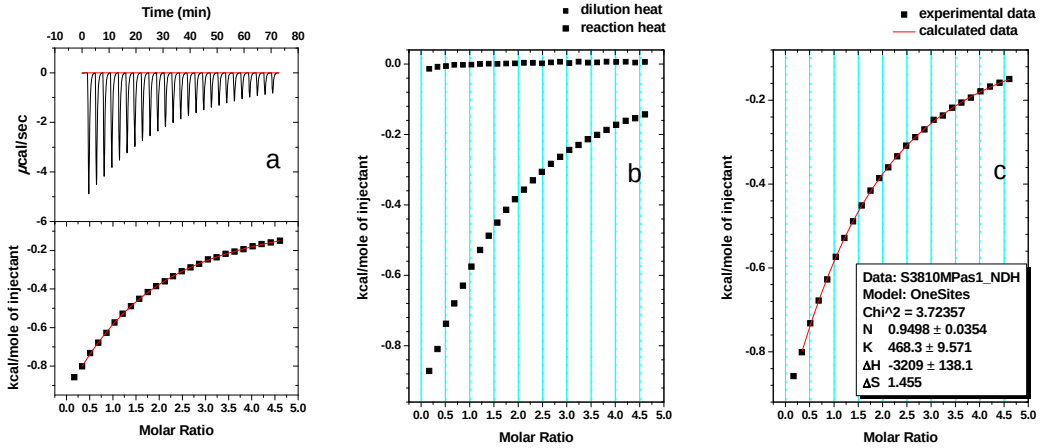

Figure S30. Calorimetric titrations for sequential 25 injections (10 μL per injection) of **6**·Br solution (21.30 mM) injecting into Na_4·**2** solution (1.036 mM): (a) raw data and apparent reaction heat; (b) heat effects of the dilution and of the complexation reaction; (c) "Net" heat effects fitted using the "one set of binding sites" model.

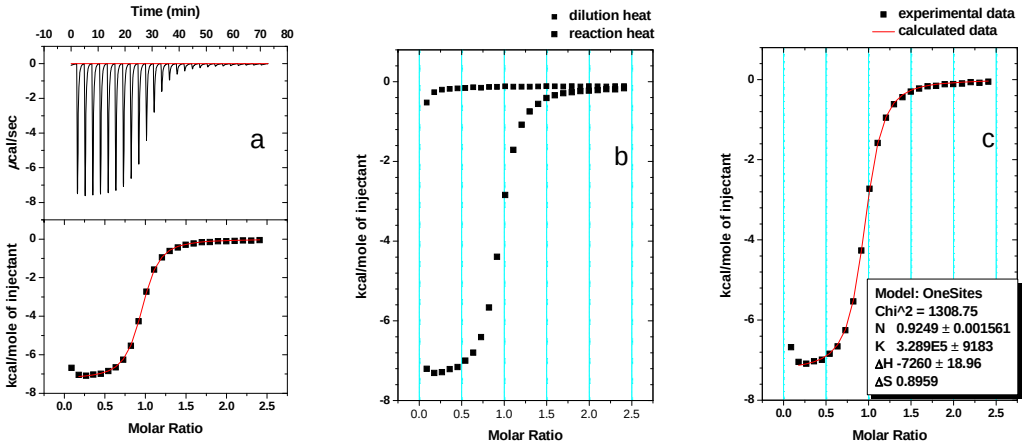

Figure S31. Calorimetric titrations for sequential 25 injections (10 μL per injection) of **3**·Br_2 solution (3.153 mM) injecting into Na_4·**2** solution (0.2502 mM): (a) raw data and apparent reaction heat; (b) heat effects of the dilution and of the complexation reaction; (c) "Net" heat effects fitted using the "one set of binding sites" model.

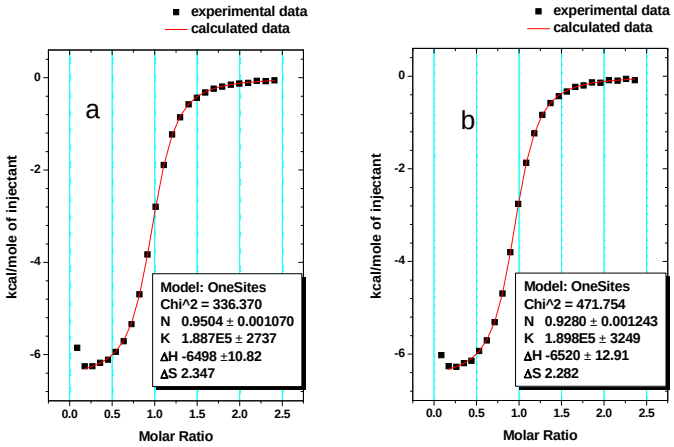

Figure S32. "Net" heat effects on complexation of **4**·Br_2 (3.153 mM) and **5**·Br_2 (3.091 mM) with Na_4·**2** (0.2502 mM) fitted using the "one set of binding sites" model: (a) **4**·Br_2; (b) **5**·Br_2.

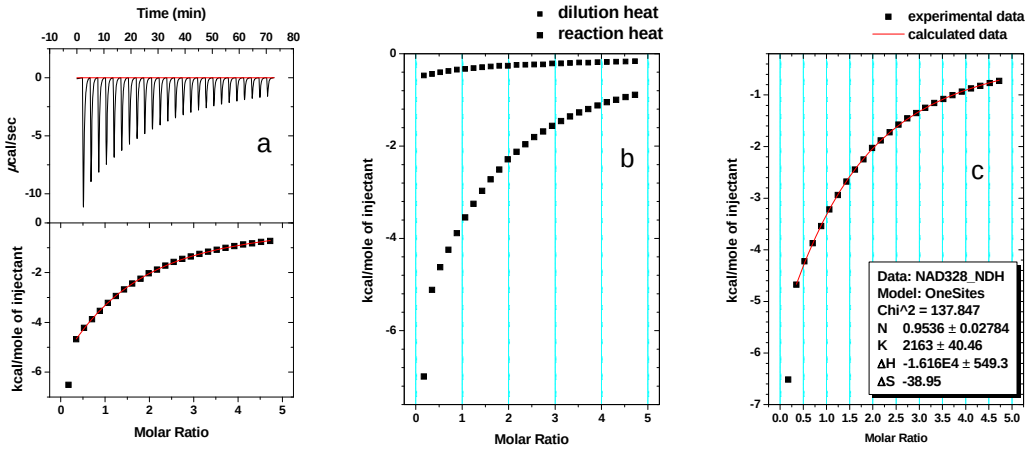

Figure S33. Calorimetric titrations for sequential 25 injections (10 μL per injection) of Na_4·**1** solution (5.926 mM) injecting into NAD^+ solution (0.2398 mM): (a) raw data and apparent reaction heat; (b) heat effects of the dilution and of the complexation reaction; (c) "Net" heat effects fitted using the "one set of binding sites" model.

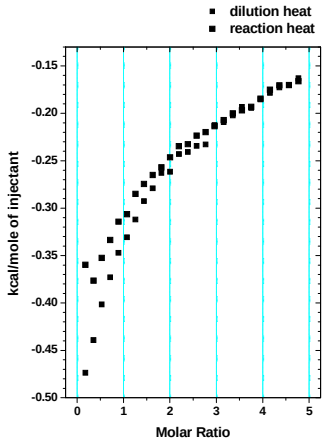

Figure S34. Heat effects of the dilution and of the complexation reaction of calorimetric titrations for sequential 25 injections (10 μL per injection): Na_4·**1** solution (5.926 mM) injecting into NADH solution (0.2482 mM).

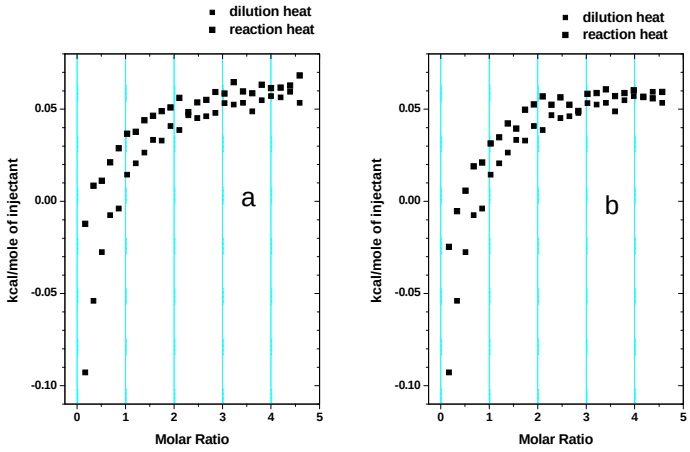

Figure S35. Heat effects of the dilution and of the complexation reaction of calorimetric titrations for sequential 25 injections (10 μL per injection): (a) Na_4·**2** solution (5.962 mM) injecting into NAD^+ solution (0.2482 mM); (b) Na_4·**2** solution (5.962 mM) injecting into NADH solution (0.2494 mM).

X-Ray Diffraction Data

3$_2$·**1**. $C_{56.50}H_{100.25}N_{4.25}O_{38.50}S_4$, crystal size 0.24 × 0.18 × 0.10 mm, triclinic, P-1, a = 12.261(3) Å, b = 23.082(7) Å, c = 28.567(8) Å, α = 108.262(4)°, β = 91.474(3)°, γ = 105.118(5)°, V = 7361(4) Å^3, z = 4, ρ_{calcd} = 1.429 g/cm^3, μ = 0.227 mm^{-1}, T = 113(2) K, 62305 measured reflections, 25909 unique reflections, 1917 parameters, 21 restraints, (R(int) = 0.0384), R_1 = 0.0570, wR_2 = 0.1564 (I>2σ(I)), R_1 = 0.0705, wR_2 = 0.1663 (all data), GoF(F^2) = 1.091.

3$_2$·**2**. $C_{60}H_{80}N_4O_{28}S_4$, crystal size 0.20 × 0.18 × 0.16 mm, orthorhombic, Pnma, a = 14.067(3) Å, b = 31.391(6) Å, c = 14.279(3) Å, V = 6305(2) Å^3, z = 4, ρ_{calcd} = 1.510 g/cm^3, μ = 0.245 mm^{-1}, T = 113(2) K, 48964 measured reflections, 7645 unique reflections, 484 parameters, 8 restraints, (R(int) = 0.0373), R_1 = 0.0413, wR_2 = 0.1031 (I>2σ(I)), R_1 = 0.0441, wR^2 = 0.1051 (all data), GoF(F^2) = 1.086.

4$_2$·**2**. $C_{66}H_{106}N_4O_{35.72}S_4$, crystal size 0.20 × 0.18 × 0.14 mm, triclinic, P-1, a = 15.794(6) Å, b = 15.349(6) Å, c = 17.438(7) Å, α = 110.9050(10)°, β = 113.174(6)°, γ = 97.646(4)°, V = 3890(3) Å^3, z = 2, ρ_{calcd} = 1.413 g/cm^3, μ = 0.216 mm^{-1}, T = 113(2) K, 33463 measured reflections, 13689 unique reflections, 1112 parameters, 106 restraints, (R(int) = 0.0518), R_1 = 0.0676, wR_2 = 0.1691 (I>2σ(I)), R_1 = 0.0942, wR_2 = 0.1897 (all data), GoF(F^2) = 1.048.